A TENSILE FRACTURE MODEL FOR ICE

S. S. Sunder and S. Nanthikesan
Massachusetts Institute of Technology
Department of Civil Engineering
Cambridge, Massachusetts

ABSTRACT

The fracture of ice under tensile loading is characterized in terms of the stress versus separation behavior in the process zone. This process zone characterization can be used in numerical simulations based on discrete crack models. The stress-separation model is then integrated with a rate-sensitive tensile stress-strain-strength model to account for strain-softening at the continuum scale. The resulting constitutive theory can be applied, in conjunction with an objective energy criterion proposed here, to simulate localized fracture processes based on the blunt crack band theory. Quantitative estimates of the fracture process zone size are obtained to assess the validity of toughness measurements based on linear elastic fracture mechanics (LEFM).

INTRODUCTION

In most real world applications involving ice either as a load bearing medium or as a load transmitting medium, the strength of ice is limited by fracture. Investigations on the fracture behavior of ice have been relatively few in comparison to the work on its continuum behavior. They include the works of Gold (1), Goetze (2), Goodman (3-5), Hamza and Muggeridge (6,7), Urabe et al. (8-10), Timco and Frederking (11,12), and Schulson and Nixon (13,14). Mellor (15) has reviewed much of this research. The general emphasis of past work has been to characterize the mode I fracture behavior of both pure and sea ice in terms of the linear elastic fracture toughness parameter, K_{Ic}, through a sequence of tests conducted under varying rates of loading and varying temperature. Since for rates of loading greater than about 10 KPa $m^{1/2}$ and temperatures below about -10°C the fracture toughness parameter K_{Ic} tends to become insensitive to rate and temperature, it is believed that LEFM applies under such conditions. Theoretical support for the loading rate criterion has been proposed by Urabe et al. (9) based on Riedel and Rice's (16) analytical study of tensile cracks in creeping solids which assumes that elastic strains dominate almost everywhere in the specimen except in a small "creep zone", which grows around the crack tip. The analysis models ice as an elastic, power law material and considers the fracture "process zone" to be of negligible size within the creep zone.

This paper is motivated by the following three concerns:

1. Numerical models for simulating fracture processes during ice-structure interaction may be developed on the basis of two distinct theories. The first theory leads to discrete crack models (17-20) which assume that all cracking activity is localized on a plane. The second theory leads to smeared or blunt crack models (21-24) which assume that cracking activity is distributed over a characteristic width representing a material property. Constitutive models describing fracture of ice under tensile loading suitable for use with either of the two numerical approaches are lacking at the present time.

2. In many practical applications, fracture in ice is accompanied by significant nonlinear viscoelastic deformations. For example, in the Arctic nearshore zone viscoelastic deformations accumulate during the winter months prior to "breakout" which occurs in early spring as a result of crack nucleation and propagation. The associated states of stress and strain in the ice tend to be multiaxial, the strains typically being tension-compression in the region where cracks nucleate (25,26). This precludes the use of LEFM-based fracture toughness parameters.

However, it is entirely possible that the fracture process zone behavior itself remains brittle while the nonfracturing parts of the material are responding in a non-brittle (nonlinearly viscoelastic) manner. This raises the following questions: (a) under what conditions is the preceding statement valid, and (b) how can this type of fracture behavior be characterized.

3. The behavior of ice is often governed by cracks that nucleate as a result of the applied stress field and which subsequently propagate. Traditionally, fracture mechanics is concerned only with propagation of pre-existing cracks in a material. Furthermore during the initial stages of crack growth, "small scale yielding" assumptions of LEFM are violated since the process zone size is comparable to the crack length. The theoretical basis and experimental data to predict the nucleation and growth history of cracks in ice is nonexistant at the present time.

This paper characterizes fracture of ice under tensile loading in terms of the stress versus separation behavior in the process zone. This process zone characterization can be used in numerical simulations based on discrete crack models. The stress-separation model is then integrated with a rate-sensitive tensile stress-strain-strength model to account for strain-softening at the continuum scale. The resulting constitutive theory can be applied, in conjunction with an objective energy criterion proposed here, to simulate localized fracture processes based on the blunt crack band theory. Quantitative estimates of the fracture process zone size are obtained to assess the validity of toughness measurements based on LEFM.

STRESS-SEPARATION MODEL OF PROCESS ZONE

The classical LEFM analysis predicts a stress singularity at the crack tip, which physically is impossible. The material in the vicinity of the crack tip must undergo inelastic deformation leading to a physically acceptable redistribution of the asymptotic stress field. The region in which such inelastic deformations occur is defined as the "process zone." In brittle materials, e.g., ice, concrete and ceramics, the width of the process zone is narrow and can be considered to have localized on the plane of the crack for fracture in the opening mode (27,28). The process zone deformation for such materials is essentially due to microcracking. The stress carrying capacity varies within the process zone (as shown in Fig. 1), from a maximum equal to the uniaxial tensile strength at the outer edge of the process zone (close to the continuum where microcracking activity is a minimum) to zero at a point where there is no traction on the faces along the crack plane. The traction free surface does not commence at the visible crack tip in general, and the value of finite crack opening distance at the zero stress point is termed the critical crack tip opening displacement or separation, δ_c.

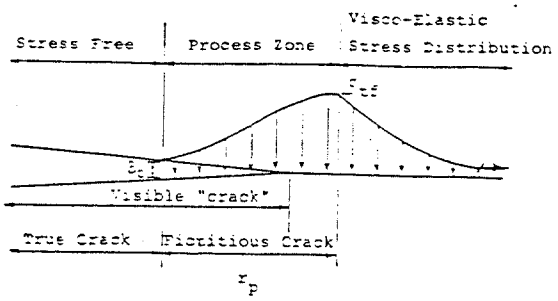

Figure 1: Fracture Process Zone Model for Ice.

The advantages of treating the process zone as part of the crack by relating the stress carrying capacity to variations in separation associated with the microcracking has been investigated by Barenblatt (29) for brittle materials, and by Hillerborg (17) and others for concrete. Rice (30) has shown that the area under the stress-separa-tion curve characterizing the behavior of the process zone is equal to the critical value of the J-integral, J_c. This value can be interpreted as the rate of energy release associated with crack extension, and under plane strain conditions is identical to the critical strain energy release rate, G_c, from an LEFM analysis. Since the fully developed process zone is independent of the loading conditions or specimen geometry, the stress-separation curve (and J_c) which characterizes it is a material property. The same cannot be said for K_{Ic} or G_c. The following statements can now be made:

(a) The single parameter characterization using J_c implies that the fracture behavior is completely defined by the process zone response and is independent of the continuum behavior of the rest of the material.

(b) The stress-separation curve can be used to characterize the strain-softening behavior of brittle materials (process of formation of a macrocrack by the localization of microcracks) under tension. Even under uniform uniaxial tensile loading conditions the microcracks are known to localize in a narrow band in brittle materials including ice, although the micromechanisms governing this phenomenon are not well understood.

(c) The experimental determination of the stress-separation curve (and from it G_c or K_{Ic}) poses no restrictions on the size of the specimens used in testing.

Determination of K_{Ic} based on a LEFM approach requires that small scale yielding (SSY) conditions be satisfied.

(d) The applicability of the stress-separation curve as a material property is strictly limited to materials in which the process zone can be approximated as having localized on the crack plane. Thus it is inappropriate for ductile materials displaying necking.

Quantfication of the stress-separation model requires knowledge of the shape of the curve, area (fracture energy, G_F), and tensile strength, σ_{tf}. The shape of the stress-separation curve is important in determining the fracture process zone development. Since experimental data is unavailable for ice at the present time, typical shapes have to be postulated based on prior experience with concrete (Fig. 2). Pure polycrystalline ice has a much more homogeneous ("uniform") microstructure than does concrete; as a result the curve is unlikely to have an elongated tail and the choice of a linear stress-separation curve may be realistic. Identical simplifying assumptions have been successfully applied to concrete (27). The critical separation distance is then given by:

$$\delta_c = 2G_F/\sigma_{tf} \qquad (1)$$

Using typical values of σ_{tf} (0.96 MPa) and G_F (1.1×10^{-3} KPa-m) corresponding to high rates of loading for ice with a grain size of 8mm, Eq. (1) yields $\delta_c = 2.3\times10^{-3}$mm. This number is smaller but in general agreement with measurements of critical crack opening displacement made on freshwater ice of approximately the same grain size by Hamza and Muggeridge (7).

The value of G_F for ice should be obtained from the area under the stress-separation curve. In the absence of experimental data for the curve, G_F may be estimated from K_{Ic} values obtained from conventional tests conducted on ice at high loading rates. Typical values of K_{Ic} lie in the range of 80-120 KPa-$m^{1/2}$ for pure ice, which leads to the value of G_F considered earlier. However, it must be realized that some of the existing data on K_{Ic} may have reduced accuracy due to inadequacies in the size of the specimens used in testing. A first order estimate of the process zone size may be obtained with the analysis of Ingraffea and Gerstle (20) which accounts for the stress redistribution ahead of the crack tip due to microcracking. Their approach, similar to Irwin's correction for plastic zone size in ductile materials (see, for example, Ref. 31), yields process zone length estimates of 4.2-8.5mm for ice with a grain size of 5mm. Specifications for K_{Ic} testing require crack and ligament lengths equal to 25 times the plastic zone size (31), which if applied to the process zone size of ice would require lengths in the range of 105-212mm or approximately 20-40 times the grain size. This approximate result is consistent with the recommendations of the IAHR

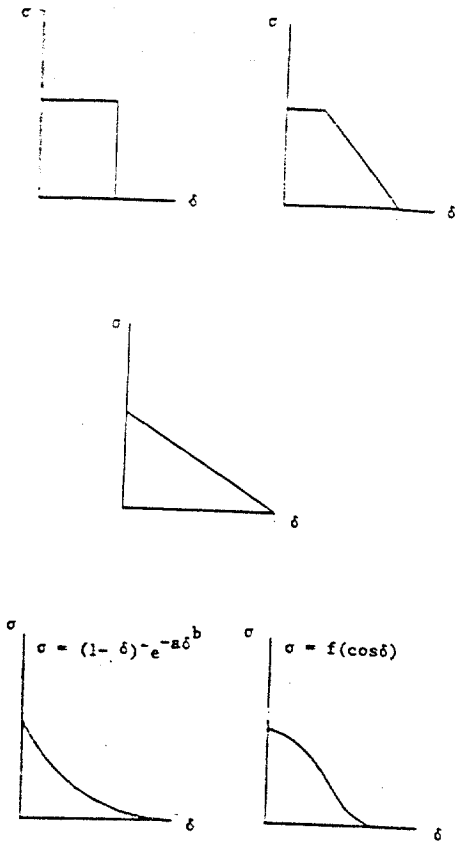

Figure 2: Typical Stress-Separation Curves.

Working Group on Testing Methods in Ice (32). In particular, the working group suggested that the lengths of the crack and the uncracked ligament should be greater than 15 times the average grain size. Typical specimen sizes used in ice testing often violate these requirements, and consequently fracture toughness estimates obtained from such tests may have reduced accuracy.

The tensile strength of ice is the higher of two stresses: the stress to nucleate cracks, σ_{tn}, and that to propagate cracks, σ_{tp}, (33,34), i.e.:

$$\sigma_{tn} = \sigma_i + kd^{-1/2} \qquad (2)$$

and

$$\sigma_{tp} = Kd^{-1/2} \qquad (3)$$

where σ_i = friction stress needed to move unlocked dislocations along the slip plane; k = measure of the resistance of grain boundaries to slip; and K represents the combined effect of fracture toughness, crack geometry, and other

micromechanical effects such as microcrack interaction and the ratio of microcrack size to and grain size. Typical values of the constants at -10°C are 0.63 MPa, 0.03 MPa-$m^{1/2}$ and 0.050 MPa-$m^{1/2}$ respectively.

The above characterization of the stress-separation curve is appropriate at high rates of loading (and low temperatures) where ice behaves as a brittle material. At lower rates (and higher temperatures) ice is in transition from brittle to ductile behavior. Here delayed elasticity or primary creep and secondary creep deformations can become significant (35,36). However, the process zone corresponds only to the localized region undergoing microcracking (or tertiary creep deformations). Thus, the tensile fracture process zone in ice may display either a purely brittle behavior insensitive to rate (and temperature) or a combination of brittle and ductile behavior that is rate (and temperature) sensitive. The profile of the stress-separation curve at the instant of loading or soon thereafter will be similar to that at high rates of loading. Over time, as the tensile strain reaches the fracture strain at lower strainrates the profile may change, i.e., the process zone size will increase if the fracture energy is constant and the tensile strength reduces. The presence of a large creep zone will invalidate laboratory measurements of K_{Ic} based on LEFM, but the stress-separation approach remains valid as long as the fracturing process is localized on a plane.

The tensile strength of ice is known to reduce as the strainrate reduces when crack nucleation governs strength (37,38). In particular, σ_i in Eq. (2) depends strongly on strainrate and temperature (39,40). At low strainrates a power law model is appropriate, while at high strainrates σ_i reaches a constant value. This variation may be expressed as:

$$\frac{1}{\sigma_i} = \frac{1}{\sigma_{im}} + \frac{1}{B\dot{\varepsilon}^{1/N}} \qquad (4)$$

where σ_{im} is the frictional resistance at high strainrates (0.63 MPa), N is the power law index for ice (N=3) and B is a temperature dependent constant given as:

$$B = B_o \exp(\Delta H/Nk'T) \qquad (5)$$

with ΔH = activation energy for the rate controlling process (0.993×10^{-19} J mol^{-1}), k' = Boltzmann's constant (1.380×10^{-23} J mol^{-1} K^{-1}) and T = temperature in degrees Kelvin. From Muguruma's data on the creep of single crystals of ice (41), B_o is deduced to be 2.95×10^{-3} MPa $s^{1/3}$. The model predicts a tensile strength of 0.71 MPa at a strainrate of 6.3×10^{-8} s^{-1} and a grain size of 5mm, which corresponds to the transition from viscoelastic flow to failure by fracture as shown in the next section. Consequently, the critical separation distance increases by a factor of 1.3 over that at very high rates for the same grain size and the process zone length increases as the square of the same factor. This result, spanning approximately five decades of strainrate, shows that the stress-separation behavior for ice is essentially rate-insensitive.

In analysis of boundary-value problems based on discrete crack models, the stress-separation curve is applied for the fracture process zone while conventional stress-strain relations are used for the rest of the material. Models of this type allow prediction of the nucleation and growth history of cracks.

SOFTENING TENSILE STRESS-STRAIN MODEL

The softening model of stress-strain behavior under tensile loading consists of three parts: a description of the viscoelastic deformations prior to failure by fracture, the tensile stress at fracture, and a characterization of the "deformations" as the stress reduces to zero from the tensile strength, i.e., the phenomenon of tensile strain-softening.

The viscoelastic flow behavior of ice in tension prior to fracture is generally considered to be identical to that under compressive loading. Hawkes and Mellor (37) justify this assumption from creep tests on ice. Ting and Shyam Sunder (35,36) have modelled this flow behavior in terms of a nonlinear generalization of the two element Maxwell fluid model consisting of an elastic spring in series with a viscous dashpot.

The elastic modulus of ice is sensitive to even "slight" variations in rate of loading (15) and cannot be taken as a constant. If the Young's modulus for ice, E, is defined to be the modulus value at very high rates of loading, then the variation of effective or apparent elastic modulus, E_{eff}, with rate may be expressed as:

$$E_{eff} = E\,[1 - r \exp(-A/E\,\dot{\varepsilon}^{1/N})] \qquad (6)$$

where $\dot{\varepsilon}$ is the strainrate, r and A are constants, and N is the power law index for ice. Equation (6) shows that the effective modulus tends to the Young's modulus (E = 9.5 GPa) as the strainrate approaches infinity. When the strainrate tends to zero, the effective modulus tends to (1-r)E, and for r equal to one, the effective modulus tends to zero. If r is zero, the effective modulus is rate-insensitive and equal to the Young's modulus. A value of r less than one is necessary to model stress relaxation, and a typical value for ice is 0.65.

The rate-sensitive spring represents recoverable strains contributed both by instantaneous elasticity and by delayed elasticity (also called primary creep). The former corresponds to deformations associated with the Young's modulus and the latter to those associated with a rate-sensitive spring with modulus equal to E_d. If the two springs are in series, then:

$$1/E_{eff} = 1/E + 1/E_d \qquad (7)$$

The nonlinear viscous dashpot represents irrecoverable strains associated with secondary creep deformations. In the case of ice, the secondary creep strainrate, $\dot{\varepsilon}_{sc}$, follows the well-known power law (42):

$$\sigma = (A/M)\ \dot{\varepsilon}_{sc}^{1/N} \qquad (8)$$

where A and N are the constants in Eq. (6), and M is a third constant approximately equal to 1400. The nonlinearity is associated with the dashpot constant $\sigma/\dot{\varepsilon}_{sc}$ which is a function of the secondary creep strainrate. The parameter A describes the creep resistance of ice and is taken to follow the Arrhenius activation energy law for temperatures below -10°C, i.e.,

$$A = A_o \exp(Q/NRT) \qquad (9)$$

where Q is the activation energy (65,000 J mol^{-1}) and R is the universal gas constant (8.314 J mol^{-1}). Sinha (43) has justified the use of a single activation energy value for characterizing both secondary creep flow and delayed elasticity. A typical value for the constant A_o equals 12.4 MPa $s^{1/3}$ corresponding to his experimental work on columnar-grained ice. For temperatures above -10°C, Mellor (15) recommends the use of the complete empirical relation derived from experiments to model temperature dependence.

The stress at which ice fractures in tension has been defined in Eqs. (2), (3), (4) and (5). The resulting strength behavior of ice is summarized in Fig. 3 assuming a grain size of 5mm. For all strainrates below a certain threshold (2.1×10^{-8} s^{-1}), ice behaves as a viscoelastically flowing material. The threshold strainrate is found by equating Eqs. (1) and (8). At the threshold strainrate (which corresponds to a stress of 0.49 MPa) and higher cracks can nucleate at stresses given by Eq. (2), but the maximum stress is still dictated by the viscoelastic deformation up to a strainrate of 6.3×10^{-8} s^{-1}. At this strainrate the stress to propagate cracks (0.71 MPa according to Eq. 3) defines the tensile strength, while the nucleation stress (Eq. 2) defines the strength for rates greater than 6.9×10^{-6} s^{-1}. The existence of a critical stress below which cracks cannot nucleate has also been suggested by other investigators, including Sinha (44). Typical stress-strain curves up to the point of maximum stress are plotted in Fig. 4 for constant strainrate loading.

Constitutive models for tensile strain-softening are developed by hypothesizing that fracture consists of a band of parallel, densely distributed microcracks with a blunt front (22-24). Although the heterogeneous microstructure of the material does not display strain-softening on fracturing (45), the phenomenon allows development of an equivalent

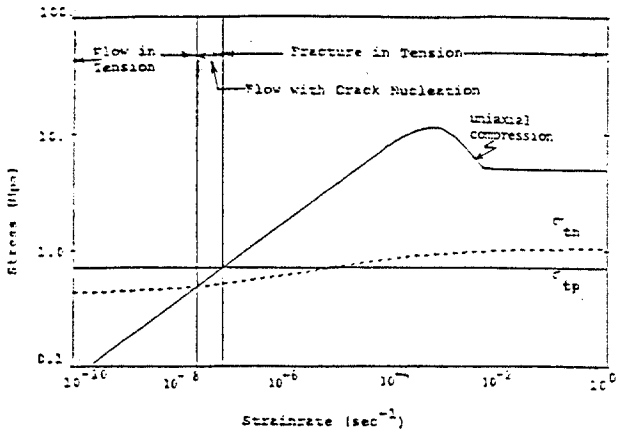

Figure 3: Domains of Pure-Ice Behavior in Tension (d=5mm)

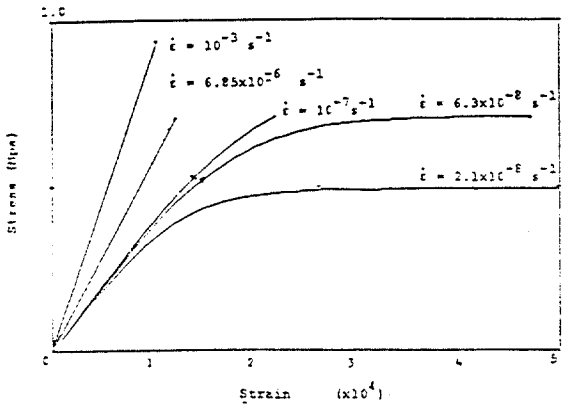

Figure 4: Tensile Stress-Strain-Strength Model for Constant Strainrate Loading (d=5mm; * indicates crack nucleation point)

homogeneous model of material behavior (46). The equivalent continuum stresses and strains are defined as the averages of the microstresses and microstrains over a certain representative volume in which the microcracking activity is confined. The cross-sectional width of this volume, w, is taken to be several (n = 1 to 20) times the size of the inhomogeneities, e.g, grain size, and represents a material property to be determined

from experiments. Extensive data correlation and analysis (23,47) yield values of n equal to 3 for concrete and 5 for rocks. Although the width of the microcrack zone may increase as the crack front extends and the density of microcracks can vary across this width, the use of a constant width with uniform distribution of microcracks suffices for most practical applications. For materials with a uniform microstructure such as pure ice the value of n tends to be small (1.5 to 3), but model predictions are relatively insensitive to variations in this value (23).

The fracture energy G_F is given as the product of the strain energy density and the width of the blunt crack band for elastic, brittle materials. This assumes that all the stored elastic energy is used locally in creating the new crack surface. However for nonlinear materials undergoing diffuse damage, for example, due to secondary creep deformations as in the case of ice, only the recoverable part of the strain energy density is available for creating new crack surfaces. The fracture energy is then the product of the recoverable strain energy density, W_F, and w, i.e.,

$$G_F = W_F\, w \qquad (10)$$

Assuming that w=nd with d=5mm and n on the order of one, a typical value for W_F is 0.22 KPa.

The tensile strain-softening profile may be related to the stress-separation curves of Fig. 2 if the localized strain across the crack band as the stress reduces to zero is taken as δ/w. For the linear stress-separation curve the critical local strain when the stress has reduced to zero is given by:

$$\varepsilon_c = 2W_F/\sigma_{tf} \qquad (11)$$

The available recoverable strain at the point of fracture or onset of instability, ε_r, is equal to:

$$\varepsilon_r = \sigma_{tf}/E_{eff} \qquad (12)$$

In theory, the evaluation of E_{eff} in Eq. (12) should be based on the unloading strainrate in the uncracked material matrix, which is equal to the total strainrate minus the local strainrate associated with the microcracking zone. However, calculations show that the matrix strainrate and the total strainrate differ by a factor of 2 to 3 and that this difference has negligible effect on the computed values of E_{eff}. The additional strain, ε_a, required for the stress to reduce from σ_{tf} to zero is equal to:

$$\varepsilon_a = \varepsilon_c - \varepsilon_r \qquad (13)$$

At high rates $\varepsilon_r = 1.12\times10^{-4}$ and $\varepsilon_a = 3.03\times10^{-4}$ while at a strainrate of 10^{-7} s^{-1} $\varepsilon_r = 1.75\times10^{-4}$ and $\varepsilon_a = 4.47\times10^{-4}$ for the linear softening model. This shows that additional strains on the order of 2.5 to 2.8 times the accumulated recoverable strains may be required for the stress to reduce to zero from the onset of instability. Values of n greater than one will lead to a reduction in the additional strains required. Typical plots of stress versus strain including the tensile strain-softening behavior are shown in Fig. 5.

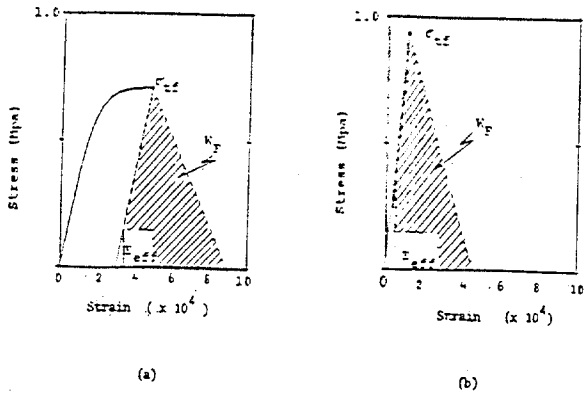

Figure 5: Softening Tensile Stress-Strain Model for Constant Strainrate Loading [d=5mm; (a): $\dot{\varepsilon}=6.85\times10^{-6}$ s^{-1}; (b): $\dot{\varepsilon}=10^{-3}$ s^{-1}]

OBJECTIVE ENERGY CRITERION

Numerical simulation of fracture processes based on tensile stress-strain models, assuming either a sudden decrease in stress at the point of failure or a gradual strain-softening region, lead to incorrect convergence properties and to results that are unobjective with respect to the choice of mesh discretization. The spurious mesh sensitivity can affect not only the post peak response of the material but also the value of maximum load (22-24). This problem can be remedied by replacing the "strength" based cracking criterion with one that preserves the "energy" dissipation required for crack propagation. Thus if the finite element size equals the width of the blunt crack band, the results from the numerical simulation will be accurate. However, an element size on the order of w (5-15mm for ice) is extremely small when considering computational efficiency. Bazant (22-24) has shown that essentially identical results can be obtained with larger elements if an objective energy criterion is applied to the tensile stress-strain relations. This criterion requires that for an element of size h, the recoverable strain energy density, W_h, should be given by:

$$G_F = W_F\, w = W_h\, h \qquad (14)$$

The tensile stress-strain relations should be modified so as to preserve W_h. For values of W_h greater than the recoverable strain energy density available at the onset of instability, W_i, i.e.,

$$W_i = \sigma_{tf}^2/2E_{eff} \qquad (15)$$

the fracture stress is kept constant, but the

softening curve is made steeper. When $w_h = w_i$, the stress drop is sudden at the point of instability. The value of h/w at which this occurs is given by:

$$(h/w)_{cr} = 2W_F E_{eff}/\sigma_{tf}^2 \qquad (16)$$

This ratio equals 3.7 at high rates and 3.5 at a strainrate of 10^{-7} s^{-1}. At larger values of h the tensile stress at fracture is reduced to σ_{tf}^h so as to preserve G_F. This requires that:

$$\sigma_{tf}^h/\sigma_{tf} = \sqrt{(h/w)_{cr}/(h/w)} \qquad (17)$$

The resulting size effect law is plotted in Fig. 6 for two strainrates. For typical element sizes that yield h/w in the range of 100 to 1000, the stress ratio in Eq. (17) varies in the range of 0.05 to 0.20. This suggests that modeling ice as a no tension material is more realistic than using a strength based fracture criterion.

$$\frac{\sigma_{tf}^h}{\sigma_{tf}} = B\left(1 + \frac{h}{Aw}\right)^{-1/2} \qquad (18)$$

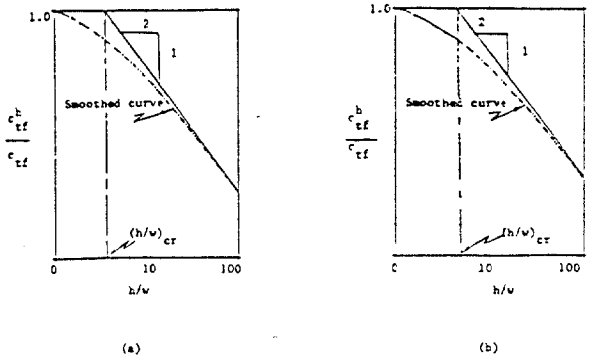

Figure 6: Size-Effect Law for Ice Under High and Low Strainrate Loading [d=5mm; (a): $\dot{\varepsilon}=10^{-7}$ s^{-1}; (b): $\dot{\varepsilon}=10^{-3}$ s^{-1}]

The discontinuous size effect law of Fig. 6 may be smoothed according to a formulation derived from dimensional analysis (48,49):

with A and B the two constants given by:

$$A = (h/w)_{cr} - 1 \qquad (19)$$

and

$$B = \left[\frac{(h/w)_{cr}}{(h/w)_{cr} - 1}\right]^{1/2} \qquad (20)$$

Note that Eq. (18) is valid only for h/w greater than or equal to unity. When h/w is exactly equal to unity the stress ratio equals one. The smoothing ensures a gradual transition from a strength based criterion to the inverse square root proportionality of an LEFM based criterion. In the transition, the fracture behavior is nonlinear. The influence of size on the tensile strength of ice in bending has also been studied by Weeks and Assur (50).

In numerical simulations based on the blunt crack band theory, the size effect law of Eq. (18) should be used to modify the tensile stress at the onset of instability or fracture. The strain-softening region should then be characterized such that it preserves the fracture energy G_F according to Eq. (14).

CONCLUSIONS

This paper has led to the development of constitutive models describing the fracture of ice under tensile loading suitable for application in numerical simulations of fracture processes based either on a discrete crack theory or on the blunt crack band theory. The models can be applied to predict the nucleation and growth history of cracks in ice as well as to characterize the process zone behavior when it remains brittle although the nonfracturing parts of the material may be responding in a non-brittle (nonlinearly viscoelastic) manner. Specific conclusions reached in the paper (in particular for ice with a grain size of approximately 5mm and the given set of material constants) are summarized below:

1. Predictions of the critical crack tip opening displacement, i.e., 2.3×10^{-4} mm, made with the stress-separation characterization of fracture behavior are somewhat smaller but in general agreement with prior experimental measurements on freshwater ice.

2. Predictions of process zone size based on a simplified analysis yield values of 4.2-8.5mm for ice. Requirements for valid measurements of fracture toughness, which stipulate crack and ligament lengths of 25 times the process zone size for ductile materials, yield values of 105-210mm (or 20 to 40 times the grain size) for ice. This result is consistent with the recommendations of the IAHR Working Group on Testing Methods in Ice requiring the dimensions to exceed 15 times the grain size. These requirements are not met by specimens often used in ice testing. Consequently, toughness estimates may have reduced accuracy.

3. The stress-separation behavior of ice is relatively insensitive to rate to loading.

4. The tensile behavior of ice consists in general of four regimes. For strainrates below a certain threshold (2.1×10^{-8} s^{-1}) ice behaves as a viscoelastically flowing material. At the threshold strainrate (which corresponds to a stress of 0.49 MPa) and higher cracks can nucleate but the maximum stress is still dictated by the viscoelastic deformation up to a strainrate of 6.3×10^{-8} s^{-1}. At this strainrate the stress to propagate cracks (0.71 MPa) defines the tensile strength, while the rate-sensitive

nucleation stress defines the strength for rates greater than 6.9×10^{-6} s^{-1}. The nucleation stress asymptotically approaches 1.06 MPa at infinite strainrate.

5. For typical finite element mesh discretizations, modeling ice as a no tension material may be more realistic than using a strength based fracture criterion.

Additional research on ice is necessary to (a) experimentally determine the stress-separation behavior and assess its rate sensitivity, (b) numerically predict its process zone size, (c) assess the possible reduction in accuracy of toughness measurements based on samples smaller than 25 times the process zone size, (d) experimentally determine the characteristic width of the crack band for ice, and (e) experimentally determine the size effect law for ice.

ACKNOWLEDGEMENTS

This research is funded by The Standard Oil Company through MIT's Center for Scientific Excellence in Offshore Engineering, and cosponsored by the U.S. Department of the Interior, Minerals Management Service.

REFERENCES

1. Gold, L.W., "Crack Formation in Ice Plates by Thermal Shocks," Canadian Journal of Physics, 41, 1963, 1712-1728.

2. Goetze, C.G., "A Study of Brittle Fracture as Applied to Ice," U.S.A CRREL, Informal Technical Note, 1965, 65p.

3. Goodman, D.J., "Creep and Fracture of Ice and Surface Strain Measurements on Glaciers and Sea Ice," Ph.D. Dissertation, University of Cambridge, England, 1977.

4. Goodman, D.J. and Tabor, D., "Fracture Toughness of Ice: A Preliminary Account of Some New Experiments," Journal of Glaciology, 21, 1978, p651.

5. Goodman, D.J., "Critical Stress Intensity Factor (K_{Ic}) Measurements at High Loading Rates for Polycrystalline Ice," Proceedings, IUTAM Symposium on Physics and Mechanics of Ice," Ed. P. Tryde, 1980, 129-146.

6. Hamza, H. and Muggeridge, D.B., "Plane Strain Fracture Toughness (K_{Ic}) of Freshwater Ice," Proceedings, POAC '79, Trondheim, Norway, 1979, 697-707.

7. Hamza, H. and Muggeridge, D.B., "Nonlinear Fracture Toughness of Freshwater Ice," Proceedings, POAC '83, Finland, 1983.

8. Urabe, N., Iwasaki,T. and Yoshitake, A., "Fracture Toughness of Sea Ice," Cold Regions Science and Technology, 3, 1980, 29-37.

9. Urabe,N. and Yoshitake, A., "Strain Rate Dependent Fracture Toughness (K_{Ic}) of Pure Ice and Sea Ice," IAHR International Symposium on Ice, Quebec, 1981, 410-420.

10. Urabe, N. et al., "Parameters on Fracture Strength of Ice," Proceedings, 1st OMAE Symposium, New Orleans, LA, 1982.

11. Timco, G.W. and Frederking, R.M.W., "Flexural Strength and Fracture Toughness of Sea Ice," Cold Regions Science and Technology, 8, 1982, 35-41.

12. Timco, G.W. and Frederking, R.M.W., "The Effects of Anisotropy and Microcracks on the Fracture Toughness (K_{Ic}) of Freshwater Ice," Proceedings, 5th OMAE Symposium, Tokyo, Japan, 1986.

13. Nixon, W.A., "The Effects of Rate, Temperature and Microstructure on the Fracture Toughness of Ice," Dartmouth College, Ice Research Laboratory, Report IRL 85/86-012, 1985.

14. Schulson, E.M. and Nixon, W.A., "The Fracture Toughness of Freshwater Ice as a Function of Temperature and Loading Rate," Proceedings, International Conference on Ice Technology, MIT, Cambridge, MA, 1986.

15. Mellor, M., "Mechanical Behavior of Sea Ice," U.S.A. CRREL, Monograph 83-1, 1983, 105p.

16. Riedel, H. and Rice, J.R., "Tensile Cracks in Creeping Solids," ASTM STP 700, 1980, 112-130.

17. Hillerborg, A., Modeer, M. and Petersson, P-E., "Analysis of Crack Formation and Crack Growth in Concrete by Means of Fracture Mechanics and Finite Elements," Cement and Concrete Research, 6, 1976, 773-782.

18. Hillerborg, A., "Analysis of Fracture by Means of the Fictitious Crack Model, Particularly for Fibre Reinforced Concrete," International Journal of Cementitious Composites, 2, 4, 1980, 177-184.

19. Pietruszczak, St. and Mroz, Z., "Finite Element Analysis of Deformation of Strain-Softening Materials," International Journal of Numerical Methods in Engineering, 17, 1981, 327-334.

20. Ingraffea, A.R. and Gerstle, W.H., "Nonlinear Fracture Models for Discrete Crack Propagation," Application of Fracture Mechanics to Cementitious Composites, NATO Advanced Research Workshop, Northwestern University, Ed. S.P. Shah, 1984.

21. Rashid, Y.R., "Analysis of Prestressed Concrete Pressure Vessels," Nuclear Engineering and Design, 7, 4, 1968, 334-355.

22. Cedolin, L. and Bazant, Z.P., "Effect of Finite Element Choice in Blunt Crack Band Analysis," Computer Methods in Applied Mechanics and Engineering, 24, 1980, 305-316.

23. Bazant, Z.P. and Oh, B.H., "Crack Band Theory for Fracture of Concrete," Materiaux et Constructions, 16, 93, 1983, 155-177.

24. Bazant, Z.P., "Mechanics of Distributed Cracking," Applied Mechanics Reviews, 39, 5, 675-705, 1986.

25. Chehayeb, F.S., Ting, S-K., Shyam Sunder, S. and Connor, J.J., "Sea Ice Indentation in the Creeping Mode," Journal of Engineering Mechanics, In Press, 1986.

26. Shyam Sunder, S., Ganguly, J., and Ting, S-K., "Anisotropic Sea Ice Indentation in the Creeping Mode," Journal of Offshore Mechanics and Arctic Engineering, In Press, 1986.

27. Petersson, P.E., "Fracture Energy of Concrete: Method of Determination," Cement and Concrete Research, 10, 1980, 79-89.

28. Mai, Y.W., "Fracture Measurements of Cementitious Composites," Applications of Fracture Mechanics to Cementitious Composites, NATO Advanced Research Workshop, Northwestern University, 1984, 399-429.

29. Barenblatt, G.I., "Mathematical Theory of Equilibrium Cracks in Brittle Fracture," Advances in Applied Mechanics, 7, 1962, 55-125.

30. Rice, J.R., "A Path Independent Integral and the Approximate Analysis of Strain Concentration by Notches and Cracks," Journal of Applied Mechanics, 1968, 379-386.

31. Broek, D., Elementary Engineering Fracture Mechanics, Martinus Nijhoff Publishers, 1986.

32. Earle, E.N., Frederking, R., Gavrilo, V.P., Goodman, D.J., Mellor, M., Petrov, I.G. and Vaudrey, K., "IAHR - Recommendations on Testing Methods of Ice," Proceedings, IAHR International Symposium on Ice, Hamburg, IV, 1984, 26-41.

33. Schulson, E.M., Lim, P.N. and Lee, R.W., "A Brittle to Ductile Transition in Ice UNder Tension," Philosophical Magazine A, 49, 3, 1984, 353-363.

34. Lee, R.W. and Schulson, E.M., , "The Strength and Ductility of Ice Under Tension," 5th OMAE Symposium, Tokyo, Japan, 1986.

35. Ting, S-K. and Shyam Sunder, S., "Constitutive Modeling of Sea Ice with Applications to Indentation Problems," Massachusetts Institutte of Technology, Department of Civil Engineering, Research Report R85-15, 1985. 255p.

36. Ting, S-K. and Shyam Sunder, S., "A Rate-Sensitive Model for the Continuum Behavior of Sea Ice," Cold Regions Science and Technology, Cold Regions Science and Technology, Submitted for Publication, 1986.

37. Hawkes, I. and Mellor, M., "Deformation and Fracture of Ice Under Uniaxial Stress, Journal of Glaciology, 11, 61, 1972, 103-131.

38. Cooksley, S.D., "Yield and Fracture Surfaces of Brittle Solids Under Multiaxial Loading," Ph.D. Thesis, Cambridge University Engineering Department, Cambridge, England, 1984.

39. Dieter, G.E., Mechanical Metallurgy, McGraw-Hill Book Company, 1976.

40. Schulson, E.M., "An Analysis of the Brittle to Ductile Transition in Polycrystalline Ice Under Tension," Cold Regions Science and Technology, 1, 1979, 87-91.

41. Muguruma, J., "Effects of Surface Condition on the Mechanical Properties of Ice Crystals," Applied Physics (J. Phys. D.), Serial 2, 2, 1969, 1517-1525.

42. Glen, J.W., "The Creep of Polycrystalline Ice," Proceedings, Royal Society of London, Series A, 228, 1175, 1955, 519-538.

43. Sinha, N.K., "Rheology of Columnar-Grained Ice," Experimental Mechanics, 18, 12, 1978, 464-470.

44. Sinha, N.K., "Delayed Elastic Strain Criterion for First Cracks in Ice," Proceedings, IUTAM Symposium on Deformation and Failure of Granular Materials, Delft, 1982, 323-330.

45. Read, H.E. and Hegemier, G.A., "Strain-Softening of Rock, Soil, and Concrete - A Review Article," Mechanics of Materials, 1984.

46. Task Committee on Concrete and Masonry Structures, ASCE State-of-the-Art Report on Finite Element Analysis of Reinforced Concrete, ASCE, New York, 1981.

47. Bazant, Z.P. and Oh, B.H., "Rock Fracturing Via Strain-Softening Finite Elements," Journal of Engineering Mechanics, 110, 7, 1984, 1015-1035.

48. Bazant, Z.P., Kim, J-K. and Pfeiffer, P., "Determination of Nonlinear Fracture Parameters from Size Effect Tests," Application of Fracture Mechanics to Cementitious Composites, NATO Advanced Research Workshop, Northwestern University, 1984.

49. Bazant, Z.P. and Kim, J-K., "Fracture Theory for Nonhomogeneous Brittle Materials with Application to Ice," Proceedings, ARCTIC '85 - Civil Engineering in the Arctic Offshore, ASCE, San Francisco, 917-930.

50. Weeks, W.F. and Assur, A., "Fracture of Lake and Sea Ice," Chapter 12 in Fracture, Ed. H. Liebowitz, VII, 1971, 879-978.